Synthesis, Structure, and Physicochemical Properties of ((Ethylsulfanyl)porphyrazinato)cobalt(II). Metal−Ligand Bonds in Co(OESPz) and in Related Cobalt(II) Tetrapyrroles: Insights from a Density Functional Study

Giampaolo Ricciardi* and Angela Rosa*

Dipartimento di Chimica, Università della Basilicata, Via N. Sauro 85, 85100 Potenza, Italy

Ilaria Ciofini

Institute of Inorganic and Analytical Chemistry, University of Fribourg, Pérolles, 1700 Fribourg, Switzerland

Alessandro Bencini

Dipartimento di Chimica, Università di Firenze, Via Maragliano 77, 50144 Firenze, Italy

Received September 25, 1998

The Co(OESPz) complex crystallizes in space group $P2_1/n$, with $a = 10.260(5)$ Å, $b = 22.650(5)$ Å, $c = 16.720(5)$ Å, $\beta = 91.680(5)°$, and $Z = 4$ and forms, similarly to the isomorphous Mn(OESPz), solid-state extended one-dimensional aggregates where "ruffled" molecular units are held together by extra planar Co···S interactions. The complex, which contains a low-spin Co^{2+} ($S = {}^1/_2$) ion, exhibits intermolecular ferromagnetic interactions ($\Theta = 2.6$ K, $g = 2.44$) propagated through a superexchange pathway by extra planar Co···S interactions, with a possible contribution of the π system. Co(OESPz) shows a Co−N_p distance shorter than CoOEP and CoPc and a sensible electrochemical stabilization of the Co^{2+} vs Co^{3+} state. The bonding interactions between Co^{2+} and the macrocyclic ligands $OMSPz^{2-}$, Pc^{2-}, Pz^{2-}, and P^{2-} are analyzed in detail, within the density functional (DF) theory, to elucidate the effects of the ligand framework. It is concluded that the σ interactions, which are by far dominant in all members of the Co^{II} tetrapyrrole series, in the aza-bridged complexes, particularly in CoPz and Co(OMSPz), are stronger than in CoP, due to the reduced "hole" size of the macrocycle. The π interactions, consisting of π back-donation from Co-3d_π into empty ring π orbitals and donation from the occupied ring π orbitals into the Co-4p_z are rather weak, but there is a sizable contribution from polarization of the macrocyclic ligand. The aza bridges have little effect on the metal to ligand π back-donation which in Co(OMSPz) is completely absent; the peripheral substituents, which are responsible for large polarization effects, play a more relevant role in the metal−macrocycle π interactions. In all porphyrazines the total orbital interaction contribution (covalent component) prevails over the ionic component of the bond, the latter being identified as the sum of the Pauli repulsion and the attractive electrostatic interaction between Co^{2+} and the tetrapyrrole(2−).

Introduction

Transition metal porphyrazines peripherally substituted with thioether groups are a new interesting class of complexes.[1] They conjugate, indeed, the peculiar electronic and structural properties of porphyrazines with the peripheral coordinating capability of the $(alkylS)_8$ cage.[1] A schematic view of a typical substituted porphyrazinato complex is shown in the Chart 1.

There are relevant questions about the coordination properties of the (alkylsulfanyl)porphyrazine ligand that merit addressing.[2] In the first place there is the fundamental question of the role played by aza bridges in determining some peculiar properties of the porphyrazine complexes, i.e., the considerable contraction of the M−N_p bond lengths (these are much shorter than in porphyrin and even slightly shorter than in the more closely related phthalocyanine complexes), the unusual ground spin states, and the electrochemical stabilization of the 2+ vs 3+ oxidation state of the coordinated first-row transition metal.[1,3]

The most common explanation is that the aza substitution strengthens both the ligand to metal σ donation and the metal to ligand π back-donation.[3,4]

(1) (a) Kobayashi, N. In *Phthalocyanines, Properties and Applications*; Leznoff, C. C., Lever, A. B. P., Eds.; VCH: New York, 1993; Vol. 2, p 97. (b) Bonosi, F.; Ricciardi, G.; Lelj, F.; Martini, G. *J. Phys. Chem.* **1993**, *97*, 9181. (c) Bonosi, F.; Ricciardi, G.; Lelj, F.; Martini, G. *J. Phys. Chem.* **1994**, *98*, 10613. (d) Ricciardi, G.; Bencini, A.; Bavoso, A.; Rosa, A.; Lelj, F. *J. Chem. Soc., Dalton Trans.* **1996**, 3243. (e) Ricciardi, G.; Bencini, A.; Bavoso, A.; Rosa, A.; Lelj, F. *J. Chem. Soc., Dalton Trans.* **1996**, 2799. (f) Ricciardi, G.; Bencini, A.; Bavoso, A.; Belviso, S.; Lelj, F. *J. Chem. Soc., Dalton Trans.* **1998**, 1985. (g) Ristori, S.; Rossi, S.; Ricciardi, G.; Martini, G. *J. Phys. Chem. B* **1997**, *101*, 8507. (h) Ricciardi, G.; Belviso, S.; Ristori, S.; Lelj, F. *J. Porphyrins Phthalocyanines* **1998**, *2*, 177. (i) Preliminary report of this paper: Ricciardi, G.; Rosa, A.; Lelj, F.; Ciofini, I.; Giannasi, E.; Bencini, A. In *Book of Abstracts*; 4th European Mediterranean Conference in Inorganic Chemistry; Corfù, Greece, 1997; University of Ioannina: Ioannina, Greece; ORC 18.

(2) Abbreviations: M, metal; Pz^{2-}, $OESPz^{2-}$, $OMSPz^{2-}$, Pc^{2-}, P^{2-}, and OEP^{2-}, dianions of a general porphyrazine, 2,3,7,8,12,13,17,18-octakis(ethylsulfanyl)-5,10,15,20-porphyrazine, 2,3,7,8,12,13,17,18-octakis(methylsulfanyl)-5,10,15,20-porphyrazine, phthalocyanine, general porphyrin, and 2,3,7,8,12,13,17,18-octaethylporphyrin; $(SALen)^{2-}$, salicylethylenediaminato dianion; near-IR, near-infrared; THF, tetrahydrofuran; DMF, *N*,*N*′-dimethylformamide.

10.1021/ic9811547 CCC: $18.00 © 1999 American Chemical Society
Published on Web 03/10/1999

Chart 1

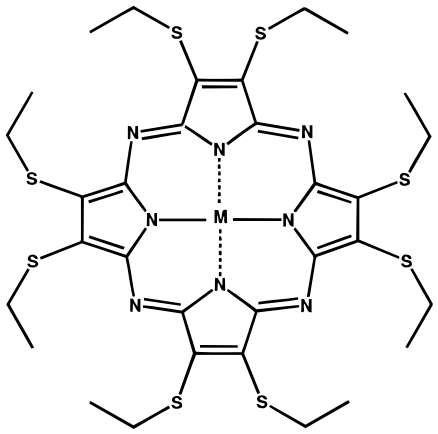

The arguments given to substantiate this view are the following: (i) The contraction of the azamethine bridge angle, probably caused by steric requirements of the lone pair electrons on the azamethine nitrogens, reduces the "hole" size of the macrocycle (the trans-N_p lies in porphyrazines ~0.2 Å closer than in porphyrins) making porphyrazines (and phthalocyanines) stronger σ-donors than porphyrins. (ii) The aza substitution of methinic groups in the porphyrin skeleton also improves the π-acceptor capability of the macrocycle by stabilizing the π-acceptor e_g* orbital.

In the second place, there is the more specific question of the effects of the peripheral thioether groups on the coordination chemistry of the (alkylsulfanyl)porphyrazines. There are indeed reasons to believe that the alkylsulfanyl substituents induce significant modifications on the electronic structure of the macrocycle.

As a matter of fact, although (alkylsulfanyl)porphyrazine complexes share with the unsubstituted metalloporphyrazines structural, redox, and magnetic properties, they show peculiar electronic spectra and chemical reactivity.[1,5]

The present work forms part of a systematic study on the coordination properties of first-row transition metal (ethylsulfanyl)porphyrazines and deals specifically with the case of cobalt(II) derivative of (ethylsulfanyl)porphyrazine, Co(OESPz), of which we present a combined experimental and theoretical characterization on the basis of the density functional (DF) theory.

To throw light on the questions outlined above we have investigated the structural, electrochemical, spectroscopic, and magnetic properties of this complex in comparison with those of a peripherally substituted porphyrin, CoOEP, and of a well-studied tetraazapyrrole complex, CoPc.

The effects of introducing aza bridges onto the porphyrin skeleton and of introducing peripheral substituents such as $(alkylS)_8$ cage and benzo rings in tetraazaporphyrins on the electronic structure and bonding properties of the systems have been elucidated through density functional calculations on the following series of cobalt(II) complexes: CoP; CoPz; CoPc; Co(OESPz). Special emphasis has been devoted to the study of the metal−macrocycle interactions in these Co^{II} tetrapyrrole complexes. Extensive use of an energy decomposition scheme (see next section) has been made which, combined with a fragment formalism, has been proven to be a useful tool in the analysis of the bonding mechanism in other porphyrin-like compounds.[6]

This scheme allows us to separate ionic (steric factors) and covalent (orbital interactions) contributions to the bonding energy. The latter are broken up according to the irreducible representations of the point group (D_{4h}), which affords a quantitative estimate of the strength of σ and π interactions. It is a well-known result of EPR spectroscopy that the ground state of square-planar and square-pyramidal low-spin Co(II) complexes is a rather complicated admixture of Slater determinants which arise from the possible distributions of the unpaired electron among the nearly degenerate d_{xy}, d_{xz}, d_{yz}, and d_{z^2} orbitals.[7] This ground state cannot be accounted for in standard DF calculations, and we have been forced to use a single determinant picture of the ground state of the complexes. This approximation was already used to analyze the metal−ligand bonding interactions in other macrocyclic complexes,[6] and as a matter of fact, the DF description of the ground state of CoSALen afforded g and A values in nice agreement with experimental EPR data.[8]

Experimental Section

Materials. All chemicals and solvents (Aldrich Chemicals Ltd.) were of reagent grade and used in the syntheses as supplied. Solvents used in physical measurements were of spectroscopic or HPLC grade. Anhydrous $CoBr_2$ was obtained from Strem. Anhydrous ethanol, DMF, and THF were obtained according to the procedures described in the literature.[9] Silica gel used for chromatography was Merck Kieselgel 60 (270−400 mesh). $(TBA)ClO_4$ (tetrabutylammonium perchlorate) was recrystallized from ethanol and dried under mild vacuum. Air- and moisture-sensitive chemicals were handled under an inert nitrogen atmosphere using standard Schlenk techniques or in a homemade glovebox.

Physical Measurements. Microanalyses were performed at the Butterworth Laboratories Ltd., Teddington, Middlesex, U.K. Fast atom bombardment mass spectra (FAB MS) were recorded on a VG ZAB 2SE double-focusing mass spectrometer equipped with a cesium gun operating at 25 kV (2 mA) using a 3-nitrobenzyl alcohol (NBA) matrix. Solution electronic spectra in 1 or 10 cm path length quartz cells in the region 200−2500 nm were performed on a UV−vis−NIR Cary 05E spectrophotometer, and proton ^1H NMR spectra, on an Bruker AM 300 MHz spectrometer. Polycrystalline powder EPR spectra have been measured in the temperature range 4.2−300 K using a Varian E-9 spectrometer. Liquid-helium temperature was reached with an ESR90 cryostat (Oxford Instruments). Variable temperature magnetic measurements have been performed in the temperature range 2.5−270 K using a Metronique Ingegnierie SQUID apparatus. Electrochemical measurements were performed with an EG&G Princeton Applied Research (PAR) potentiostat/galvanostat, Model 273, or with an AMEL 5000 System, in conjunction with a Linseis X-Y recorder; for all readings a three-electrode system in THF or DMF containing 0.1 M of supporting

(3) (a) Fitzgerald, J. P.; Haggerty, B. S.; Rheingold, A. N.; May, L. *Inorg. Chem.* **1992**, *31*, 2006. (b) Yaping, N.; Fitzgerald, J.; Carroll, P.; Wayland, B. B. *Inorg. Chem.* **1994**, *33*, 2029. (c) Ghosh, A. J.; Fitzgerald, J.; Gassman, P. G.; Almlof, J. *Inorg. Chem.* **1994**, *33*, 6057. (d) Fitzgerald, J. P.; Yap, J. P. A.; Rheingold, A. L.; Brewer, C. T.; May, L.; Brewer, G. A. *J. Chem. Soc., Dalton Trans.* **1996**, 1249.
(4) Boucher, L. J. In *Coordination Chemistry of Macrocyclic Compounds*; Melson, G. A. E., Ed.; Plenum Press: New York, 1979; p 527 and references therein.
(5) Ricciardi G.; et al. *Inorg. Chem.*, submitted for publication.
(6) (a) Rosa, A.; Baerends, E. *Inorg. Chem.* **1993**, *32*, 5637. (b) Rosa, A.; Baerends, E. *Inorg. Chem.* **1994**, *33*, 584. (c) Rosa, A.; Ricciardi, G.; Rosi, M.; Sgamellotti, A.; Floriani, C. *J. Chem. Soc., Dalton Trans.* **1993**, 3759. (d) Rosa, A.; Baerends, E. *Inorg. Chem.* **1992**, *31*, 4717.
(7) Daul, C.; Schläpfer, C. W.; von Zelewsky, A. *Struct. Bonding* **1979**, *36*, 129.
(8) Daul, C.; Bruyndonckx, R. Private communication and manuscript in preparation.
(9) Perrin, D. D.; Armarego, W. L. F. *Purification of laboratory chemicals*, 3rd ed.; Pergamon Press: Oxford, U.K., 1988.

Table 1. Crystallographic Data for Co(OESPz)

empirical formula	$C_{32}H_{40}CoN_8S_8$
fw	852.13
temp	293(2) K
wavelength	1.541 84 Å
cryst system	monoclinic
space group	$P2_1/n$
unit cell dimens	$a = 10.260(5)$ Å, $\alpha = 90.000(5)°$ $b = 22.650(5)$ Å, $\beta = 91.680(5)°$ $c = 16.720(5)$ Å, $\gamma = 90.000(5)°$
V	3884(2) Å^3
Z	4
D (calcd)	1.457 g/cm^3
abs coeff	0.908 mm^{-1}
cryst size	0.6 × 0.03 × 0.08 mm
goodness-of-fit on F^2	1.143
final R indices [$I > 4\sigma(I)$][a]	$R_1 = 0.0974$; w$R_2 = 0.2134$

[a] $R_1 = [\sum||F_o| - |F_c||/\sum|F_o|]$; w$R_2 = \{\sum[w(F_o^2 - F_c^2)^2]/\sum[wF_c^4]\}^{1/2}$.

electrolyte ((TBA)ClO_4) was employed. Cyclic voltammetric measurements were obtained with a double platinum electrode and a SCE reference electrode equipped with a Luggin capillary under an atmosphere of purified N_2. Redox potentials obtained were corrected by the potential of a ferrocenium/ferrocene couple (0.437 and 0.457 V in THF and DMF, respectively). The same correction was applied to literature data for the sake of comparison.

Syntheses. The free porphyrazine, $OESPzH_2$, was synthesized using the procedure already described in the literature.[1h] Anal. Calcd (found) for $C_{32}H_{42}N_8S_8$: C, 48.25 (48.33); H, 5.27 (5.32); N, 14.01 (14.09); S, 32.15 (32.26). ^{1}H NMR (δ/ppm): δ_H (300 MHz, $CDCl_3$) −0.95 (2 H), 1.52 (24 H, t), 4.25 (24 H, q). Electronic spectrum in CH_2Cl_2 [λ_{max} (log ϵ)]: 360 (4.67); 490 (4.17); 520 (4.18); 632 (4.58), 670 (4.56 sh), 655 (4.60), 715 (4.81). FAB-MS (NBA matrix, positive ion mode): $m/z = 794$, cluster, $M^+ - H$ (calcd $m/z = 794$).

Co(OESPz). $CoBr_2$ (0.040 g, 0.183 mmol) was dissolved in a stirred, hot solution of $OESPzH_2$ (0.100 g, 0.125 mmol) in 1:1 1,4-dioxane/EtOH mixture (25.0 mL) at the reflux temperature. Within 15 min no unmetalated porphyrazine was present as indicated by UV/vis spectroscopy. After cooling, the solvent mixture was rotary evaporated, and the resulting deep blue solid was passed through a column of silica gel using a 9:1 CH_2Cl_2/EtOH mixture as eluant. Reduction of the solvent volume under vacuum caused black, needlelike crystals to form. These were collected by filtration and air-dried. Recrystallization by slow evaporation of the solvent from a 7:3 CH_2Cl_2/EtOH mixture gave 0.125 g (~100%) of pure product in the form of well-shaped black needles. Anal. Calcd (found) for $C_{32}H_{40}CoN_8S_8$: C, 45.10 (44.91); H, 4.70 (4.28); N, 13.13 (12.94). Electronic spectrum in C_6H_6 [λ_{max} (log ϵ)]: 360 (4.67); 490 (4.17); 520 (4.18); 632 (4.58), 670 (4.56 sh), 655 (4.60), 715 (4.81).

Crystallography. X-ray-quality crystals of Co(OESPz) in the form of thin, black needles were grown by very slow evaporation of EtOH solutions of the complex. Attempts to prepare X-ray-quality crystals by evaporation of CH_2Cl_2 or $CHCl_3$ solutions of Co(OESPz) led to the formation of apparently well-shaped needlelike crystals that were found to be composed by bundles of fibers at a preliminary X-ray investigation. A summary of crystal data, data collection, and refinement parameters for Co(OESPz) is given in Table 1, and atomic coordinates are given in Table 2.

All data were collected at room temperature on an Enraf Nonius CAD-4 diffractometer using graphite-monochromatized Cu Kα radiation. The unit cell was determined from 25 well-centered reflections. The intensity data were collected in an $\omega-2\theta$ scan mode. A total of 7124 reflections were measured to $\theta_{max} = 69°$; 3601 reflections with $I > 4\sigma(I)$ were used. Data reduction included correction for background and Lorentz−polarization effects.[10] Absorption correction was applied according to ref 11. The intensities of two reflections were measured every 1 h during data collection as a check of the stability of the diffractometer and the crystal; no appreciable decay of the intensities was observed during data collections. The crystal orientation was checked every 200 intensity measurements using two control reflections.

Table 2. Atomic Coordinates (×10^4) and Equivalent Isotropic Displacement Parameters (Å^2 × 10^3) for Co(OESPz)

	x	y	z	U(eq)[a]
Co(1)	2591(2)	193(1)	6159(1)	49(1)
S(1)	3004(3)	−530(1)	2926(2)	50(1)
S(2)	5722(3)	−1149(1)	3998(2)	44(1)
S(3)	6590(3)	1410(1)	7055(2)	50(1)
S(4)	5714(3)	−567(2)	8885(2)	57(1)
S(5)	2711(3)	1203(2)	9277(2)	62(1)
S(6)	342(3)	2034(2)	8016(2)	59(1)
S(7)	−1651(3)	1708(1)	5114(2)	47(1)
S(8)	−973(3)	797(1)	3545(2)	44(1)
N(1)	3159(7)	−220(3)	5260(4)	28(2)
N(2)	4910(8)	−813(4)	5835(4)	36(2)
N(3)	3882(7)	−195(3)	6805(4)	29(2)
N(4)	3557(8)	259(4)	8086(4)	35(2)
N(5)	2072(7)	637(3)	7058(4)	34(2)
N(6)	409(7)	1263(3)	6459(4)	31(2)
N(7)	1284(7)	576(3)	5518(4)	31(2)
N(8)	1632(8)	126(4)	4237(4)	35(2)
C(1)	2661(9)	−187(4)	4488(5)	32(2)
C(2)	3375(9)	−539(4)	3949(5)	33(2)
C(3)	4396(9)	−797(4)	4393(5)	31(2)
C(4)	4190(9)	−610(4)	5222(5)	32(2)
C(5)	4705(9)	−625(5)	6565(5)	33(2)
C(6)	5474(9)	−865(4)	7262(6)	35(2)
C(7)	5085(10)	−564(5)	7902(6)	40(3)
C(8)	4083(10)	−139(5)	7625(6)	38(2)
C(9)	2667(9)	637(4)	7812(5)	31(2)
C(10)	2141(10)	1098(5)	8298(6)	40(3)
C(11)	1238(10)	1402(4)	7825(6)	38(2)
C(12)	1207(10)	1098(5)	7064(6)	37(2)
C(13)	457(9)	1002(4)	5749(6)	34(2)
C(14)	−441(9)	1163(4)	5085(6)	34(2)
C(15)	−103(9)	827(4)	4449(6)	34(2)
C(16)	987(10)	467(4)	4726(5)	35(2)
C(17)	3220(18)	−1249(6)	2579(8)	103(6)
C(18)	3045(18)	−1270(8)	1693(8)	111(6)
C(19)	6412(13)	−1639(5)	4743(7)	60(3)
C(20)	5556(48)	−2153(23)	5025(16)	61(10)
C(20A)	5620(71)	−2158(30)	4708(23)	121(24)
C(21)	7114(16)	−1698(7)	7986(7)	93(6)
C(22)	8107(16)	−2157(7)	7861(10)	120(7)
C(23)	4298(16)	−636(7)	9483(7)	84(5)
C(24)	3510(18)	−1172(9)	9302(10)	117(7)
C(25)	1276(19)	1338(9)	9802(9)	115(7)
C(26)	330(22)	840(12)	9772(12)	184(13)
C(27)	1617(17)	2559(6)	8206(10)	96(6)
C(28)	2503(23)	2667(9)	7516(13)	150(9)
C(29)	−645(14)	2365(6)	5190(8)	76(4)
C(30)	254(15)	2444(7)	4481(10)	94(5)
C(31)	143(11)	517(6)	2816(6)	55(3)
C(32)	−421(14)	634(6)	1985(6)	77(4)

[a] U(eq) is defined as one-third of the trace of the orthogonalized $\mathbf{U}_{ij}$ tensor.

Structure Analysis and Refinement. The structure was solved by direct methods using the SIR92 package. A good starting set of atomic parameters for the cobalt atom was obtained. All the other non-hydrogen atoms were located from successive Fourier and difference Fourier syntheses using the SHELXL-93 package.[12,13]

The structure was refined by full-matrix least-squares procedure based on the minimization of the function $\sum w(|F_o| - |F_c|)^2$, where the weights w were taken as $w = 1/[\sigma^2F_o^2 + (0.0517P)^2 + 31.243P]$ and P is defined as $P = (\max(F_o^2,0) + 2F_c^2)/3$.

All data were included. For all non-hydrogen atoms anisotropic thermal parameters were used. Hydrogen atoms were introduced in calculated position as idealized atoms keeping into account the proper carbon hybridization. The isotropic thermal factor for every hydrogen atom was fixed to $^3/_2$ of the corresponding carbon atom's U_{eq}. All the

(10) Walker, N.; Stuart, D. *Acta Crystallogr., Sect. A* **1983**, *39*, 159.
(11) *International Tables for X-ray Crystallography*; Kynoch Press: Birmingham, England, 1974; Vol. IV, p 99.

terminal $-CH_3$ groups of the thioethyl chains were found to be affected by thermal motion disorder. We solved the disorder by assigning the methyl carbon atom (C20) to two equivalent position (C20 and C20a) with a fixed occupancy factor of 50%. At convergence, the discrepancy indices for the Co(OESPz) are $R_1 = 0.0974$ and $wR_2 = 0.2444$ for 3601 observed data based on $I > 4\sigma(I)$ and 451 parameters. The highest peak in the last difference Fourier map was 0.497 e $Å^{-3}$.

Computational Details. The calculations reported in this paper are based on the Amsterdam DF program package[14] characterized by the use of a density fitting procedure to obtain accurate Coulomb and exchange potentials in each SCF cycle,[14e] by accurate and efficient numerical integration of the effective one-electron Hamiltonian matrix elements[15b,c] and by the possibility to freeze core orbitals.[14a]

A double-ζ STO basis set augmented by a single STO d orbital was employed for sulfur, carbon, and nitrogen atoms. The 3d, 4s, and 4p shells of cobalt were represented by a triple-ζ basis. The cores (Co, 1s−2p; C, 1s; N, 1s; S, 1s−2p) have been kept frozen.

The density functionals included Becke's[15] gradient corrections to the local exchange expression and Perdew's[16] gradient corrections to the LDA expression (VWN parametrization[17] of the electron gas data).

The geometrical parameters used for Co(OESPz), CoPc, and CoOEP have been derived from the experiments (present work, ref 18) with appropriate averaging of bond angles and bond lengths to maintain D_{4h} symmetry. In the case of CoPz for which structural data are not available, we have assumed the same geometrical parameters as for Co(OESPz). To make the calculations tractable the ethylsulfanyl groups in Co(OESPz) have been replaced by methylsulfanyl groups and the ethyl groups in Co(OEP) by hydrogen atoms. The coordinate system used in the calculations as well as the labeling of the nonequivalent atomic centers in the molecules are shown in Figure 1.

To analyze the interactions between the $OMSPz^{2-}$, Pc^{2-}, Pz^{2-}, and P^{2-} macrocycles and the metal ion Co^{2+} we use a method that is an extension of the well-known decomposition scheme of Morokuma.[19]

The interaction energy, ΔE_{int}, is split up in two physically meaningful terms (eq 1).

$$\Delta E_{int} = \Delta E^\circ + \Delta E_{oi} \quad (1)$$

ΔE°, which is appropriately called the steric repulsion,[20−22] consists of two components. The first, ΔE_{elstat}, is the classical electrostatic interaction between the unperturbed charge distributions of the interacting fragments and is usually attractive. The second component is the so-called exchange repulsion or Pauli repulsion, ΔE_{Pauli}.[23−25] This is essentially due to the antisymmetry requirement on the total wave function or, equivalently, the Pauli principle. The ΔE_{Pauli} term comprises the 3- and 4-electron destabilizing interactions between occupied orbitals on the two fragments and is responsible for the steric repulsion. The steric term ΔE° is usually repulsive at the equilibrium distance since the repulsive component ΔE_{Pauli} dominates, but for charged fragments such as Co^{2+} and tetrapyrrole(2−) the electrostatic attraction will dominate.

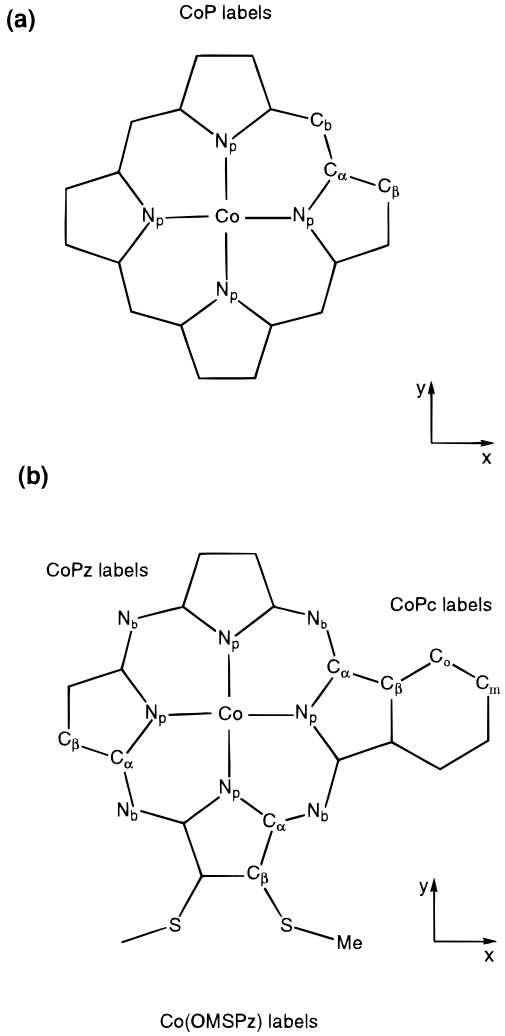

Figure 1. Atom labeling scheme for (a) CoP and (b) CoPc (right), Co(OMSPz) (bottom), and CoPz (left).

In addition to the steric term that can be identified as the ionic component of the bond, there are the attractive orbital interactions, ΔE_{oi}, that can be identified as the covalent component of the bond. This term accounts indeed for formation of electron pair bond, charge transfer (interaction between occupied orbitals on one fragment with unoccupied orbitals of the other fragment), and polarization (empty/occupied orbital mixing on one fragment).

The ΔE_{oi} term can be further split up into the contributions from the various irreducible representations G of the overall symmetry group of the system (eq 2).[26]

$$\Delta E_{oi} = \sum_\Gamma \Delta E(\Gamma) \quad (2)$$

For the evaluation of the metal−macrocycle bond energy in Co(OMSPz), we used an open-shell fragment procedure,[27] which allows for a correct evaluation of the energy terms when open-shell fragments form electron pair bonds, which is the case for Co(OMSPz) in its ^2E_g ground-state configuration (vide infra).

(12) Sheldrick, G. M. SHELXL-93, Universität Göttingen, 1993.
(13) Altomare, A.; Cascarano, G.; Giacovazzo, C.; Cuagliardi, A. *J. Appl. Crystallogr.* **1994**, *27*, 1045
(14) (a) Baerends, E. J.; Ellis, D. E.; Ros, P. *Chem. Phys.* **1973**, *2*, 42. (b) Boerrigter, P. M.; te Velde, G.; Baerends, E. J. *Int. J. Quantum Chem.* **1988**, *33*, 87. (c) te Velde, G.; Baerends, E. J. *J. Comput. Phys.* **1992**, *99*, 84. (d) Fonseca Guerra, C.; Visser, O.; Snijders, J. G.; te Velde, G.; Baerends, E. J. In *Methods and Techniques in Computational Chemistry*; Clementi, E., Corongiu, C., Eds.; STEF: Cagliari, Italy, 1995; Chapter 8, p 305.
(15) (a) Becke, A. D. *J. Chem. Phys.* **1986**, *84*, 4524. (b) Becke, A. D. *Phys. Rev.* **1988**, *A38*, 3098.
(16) (a) Perdew, J. P. *Phys. Rev.* **1986**, *B33*, 8822 (erratum: PRB 3419867406). (b) Perdew, J. P. *Phys. Rev.* **1986**, *B34*, 7406.
(17) Vosko, S. H.; Wilk, L.; Nusair, M. *J. Can. J. Phys.* **1980**, *58*, 1200.
(18) (a) Williams, G. A.; Figgis, B. N.; Mason, R.; Mason, S. A.; Fielding, P. E. *J. Chem. Soc., Dalton Trans.* **1980**, 1688. (b) Scheidt, W. R.; Turowska-Tyrk, I. *Inorg. Chem.* **1994**, *33*, 1314.
(19) Morokuma, K *J. Chem. Phys.* **1971**, *55*, 1236.
(20) (a) Ziegler, T.; Tschinke, V.; Becke, A. *J. Am. Chem. Soc.* **1987**, *109*, 1351. (b) Ziegler, T.; Tschinke, V.; Ursenbach, C. *J. Am. Chem. Soc.* **1987**, *109*, 4825. (c) Ziegler, T.; Tschinke, V.; Versluis, L.; Baerends, E. J. *Polyhedron* **1988**, *7*, 1625.
(21) Ziegler, T.; Rauk, A. *Inorg. Chem.* **1979**, *18*, 1558.
(22) Ziegler, T.; Rauk, A. *Inorg. Chem.* **1979**, *18*, 1755.
(23) Fujimoto, H.; Osamura, J.; Minato, T. *J. Am. Chem. Soc.* **1978**, *100*, 2954.
(24) Kitaura, K.; Morokuma, K. *Int. J. Quantum Chem.* **1976**, *10*, 325.
(25) Van den Hoek, P. J.; Kleyn, A. W.; Baerends, E. J. *Comments At. Mol. Phys.* **1989**, *23*, 93.
(26) Ziegler, T.; Rauk A. *Theor. Chim. Acta* **1977**, *46*, 1.
(27) Bickelhaupt, F. M.; Nibbering, N. M. M.; van Wezenbeek, E. M.; Baerends, E. J. *J. Phys. Chem.* **1992**, *96*, 4864.

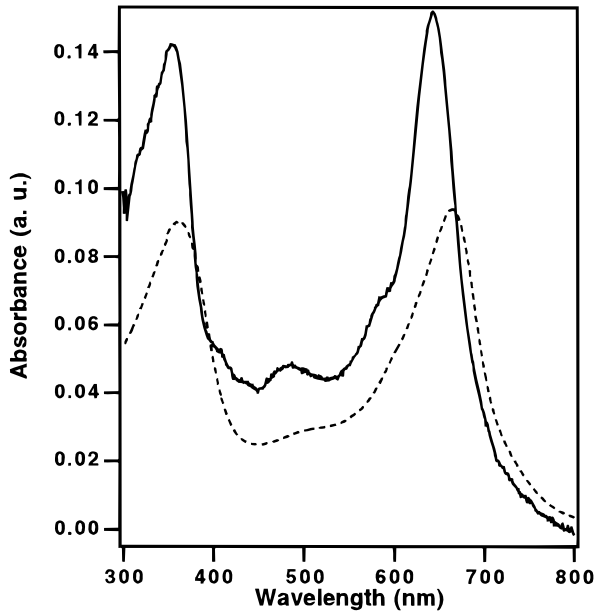

Figure 2. UV−vis absorption spectra of Co(OESPz) in benzene (solid line) ($C = 1.30 \times 10^{-6}$ M) and in 1,4-dioxane (dashed line) ($C = 2.93 \times 10^{-6}$ M).

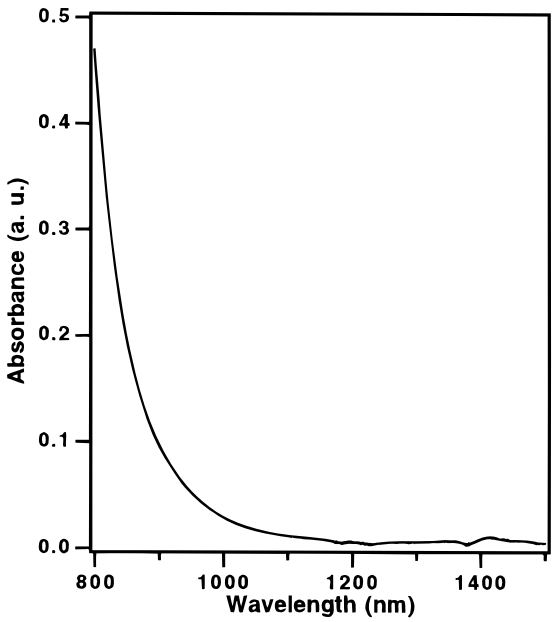

Figure 3. Near-IR absorption spectra of Co(OESPz) in benzene ($C = 3.70 \times 10^{-5}$ M).

Results and Discussion

General Properties of Co(OESPz). (a) Synthesis and Electronic Spectra. The reaction of $OESPzH_2$ with $CoBr_2$ in a 1,4-dioxane−ethanol mixture in the presence of a sterically hindered base, such as 1,2,4-trimethylpyridine, affords the complex Co(OESPz) in high yield. This can be efficiently purified by conventional chromatographic techniques. As inferred from Figure 2, where the UV−visible spectra of Co(OESPz) taken in nondonor (benzene) and in donor (1,4-dioxane) solvents are displayed, the complex shows UV−visible solution spectral features closely resembling those of the phthalocyanine analogue in that it exhibits very intense absorptions in the 600−700 and 300−400 nm regions.[28] Intense, strongly solvent-dependent absorptions are also seen in the 400−500 nm region where CoPc usually presents a window. The Soret and Q-bands are sensibly broadened relative to CoPc. This feature seems to be due to electronic effects of peripheral $(EtS)_8$ cage rather than to intermolecular aggregation processes since it is observed also at very low concentrations, even below the association limits which are 1.5×10^{-6} and 3.0×10^{-6} M in benzene and 1,4-dioxane, respectively.

Similarly to CoPc[29] and CoOEP,[30] the complex is not near-IR silent. It shows in benzene an unstructured tail absorbance that falls from $\epsilon \sim 1700$ M^{-1} cm^{-1} to the baseline between 800 and 1100 nm (see Figure 3). It can be excluded that this absorption is generated by dimerization of the complex in solution, since it is still observed at very low concentrations ($\sim 10^{-6}$ M) where the complex obeys Beer's law. At lower energy (1300−1500 nm) in the spectrum a number of bands are seen, whose intensity depends on concentration and scan rate and that must be presumed, therefore, to be vibrational in origin (peripheral C−H overtone and combination).

(b) Electrochemistry. The redox behavior of Co(OESPz) has been investigated by cyclic voltammetry in 0.1 M $(TBA)ClO_4$/THF and in 0.1 M $(TBA)ClO_4$/DMF solutions. The complex shows a fully irreversible Co(II)/Co(III) oxidation at $E_{pa} = +0.11$ V in DMF but a reversible Co(II)/Co(III) oxidation +0.34 V in THF. The potential value obtained in THF is nearly coincident with that reported for the Co(OMSPz) in the same conditions ($E_{1/2} = +0.26$).[31] To evaluate the effects of the macrocyclic framework on the Co(III)/Co(II) couple, it is useful to compare the redox behavior of Co(OESPz) with that of CoPc and CoOEP in $(TBA)ClO_4$/DMF solution. The propensity of Co(III) to form a six-coordinate species in Co(tetrapyrroles) should be, in fact, equally favored in CoPc, Co(OESPz), and Co(OEP) by the donor solvent DMF, the scarcely coordinating anion ClO_4^- playing essentially a spectator role.[31] The Co(III)/Co(II) process is reversible in CoPc and occurs at +0.03 V, being therefore only slightly cathodic of that of Co(OESPz), whereas it is fully irreversible and considerably cathodic in CoOEP ($E_{pa} = -1.51$ V).[32,33]

These data point to the remarkable capability of the (ethylsulfanyl)tetraazaporphyrinato ligand to stabilize the lower oxidation state, i.e. the 2+ vs 3+ of the coordinated metal.

(c) Structure. The molecular structure of Co(OESPz) is illustrated in the ORTEP drawing of Figure 4, which also gives the atom labels. The complex is isomorphous, although not isodimensional with Mn(OESPz). The Co(OESPz) molecules, closely held together by interactions between the cobalt atom, which lies in the plane of the four pyrrole nitrogen atoms and the sulfur atoms of two adjacent molecules, form extended one-dimensional arrays disposed in an herringbone-like fashion. The intermolecular Co−S distances (that are slightly shorter than the Mn−S ones due to the smaller size of the Co(II) ion) are alternatively 2.789(5) and 2.842(5) Å along the stack (see Figure 5), which leads to a pseudooctahedral coordination sphere around the cobalt atom. The Co−S distances are rather long.

(28) (a) Metz, J.; Schneider, O.; Hanack, M. *Inorg. Chem.* **1984**, *23*, 1065. (b) Stillman, M. J.; Thomson, A. J. *J. Chem. Soc., Faraday Trans.* **1974**, 790.
(29) Lever, A. B. P.; Pickens, P.; Minor, P. C.; Licoccia, S.; Ramaswamy, B. S.; Magnell, K. *J. Am. Chem. Soc.* **1981**, *103*, 6800.
(30) (a) Tait, C. D.; Holten, D.; Gouterman *J. Am. Chem. Soc.* **1984**, *106*, 6653. (b) Tait, C. D.; Holten, D.; Gouterman *Chem. Phys. Lett.* **1983**, *100*, 268.
(31) Bottomley, L. A.; Chiou, W. J. H. *J. Electroanal. Chem.* **1986**, *198*, 333.
(32) Beck, A.; Hanack, M.; Mangold, K. M. *Chem. Ber.* **1991**, *124*, 2315.
(33) Fuhrop, J.-H.; Kadish, K. M.; Davis, D. G. *J. Am. Chem. Soc.* **1973**, *95*, 5140.

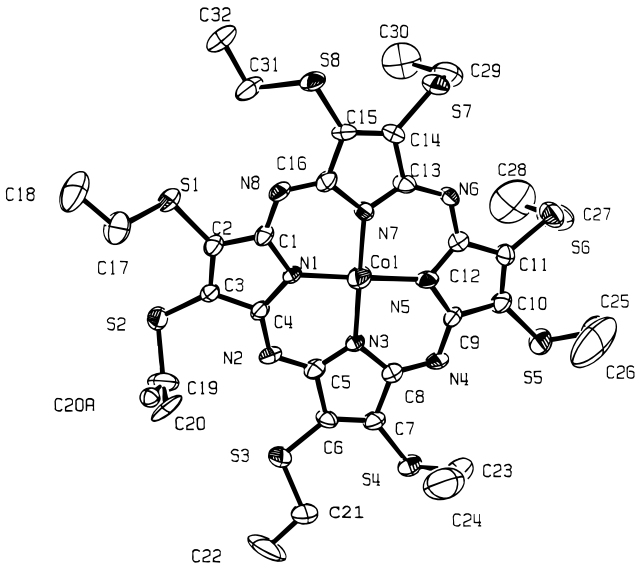

Figure 4. ORTEP diagram of Co(OESPz). Atoms are contoured at the 50% probability level. Hydrogen atoms are not shown for reason of clarity.

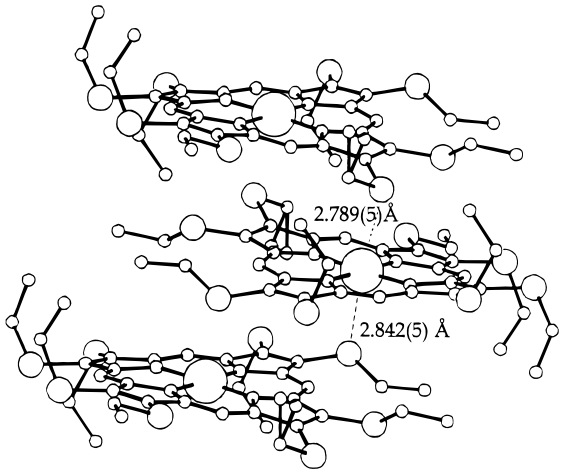

Figure 5. Edge-on view of the Co(OESPz) Co···S extraplanar interactions in the solid state. The Co···S distances shown are repeated indefinitely along the stack.

Much shorter Co−S bond lengths are generally found indeed in low-spin octahedral Co^{II}(crown thioether) complexes and in $Co^{II}N_2O_2S_2$ octahedral environments (2.249(1)−2.479(1) Å and 2.203(2)−3.105(2) Å, respectively).[34,35] As in the Mn(OESPz) parent complex, the driving force for the axial Co−S interaction to occur is provided by the axial unsaturation of the metal center.[1h] It is however the remarkable flexibility of the porphyrazineoctathiolate core (which retains a relevant structural feature of the porphyrinato ligand) that favors significantly this process. The porphyrazineoctathiolate core shows indeed, just as the very recently structurally characterized CoOEP "Sad" type[18b] S_4-ruffling that the distortion does not involve a significant up−down shift of the *meso*-nitrogen atoms with respect to the mean porphyrazinato plane and that mostly the pyrroledithiolate moieties are alternatively displaced up and down from the molecular plane (see Figure 6).

Some relevant molecular parameters of Co(OESPz) are compared with those of CoOEP and CoPc in Table 3. Three

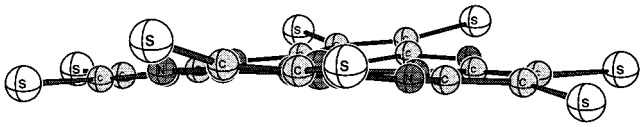

Figure 6. Stick and ball drawing illustrating the "Sad"-like ruffling of the Co−porphyrazineoctathiolato moiety of the Co(OESPz) molecule viewed down a $Co-N_p$ bond.

Table 3. Average Bond Distances (Å) and Angles (deg) for Co(OESPz), CoPc, and CoOEP

	Co(OESPz)[a]	CoPc[b]	CoOEP[c]
$Co-N_p$	1.894(7)	1.912(2)	1.971(6)
N_p-C_α	1.372(10)	1.375(4)	1.370(4)
$C_\alpha-C_\beta$	1.457(5)	1.450(5)	1.442(5)
$C_\beta-C_\beta$	1.369(7)	1.384(4)	1.360(5)
$C_\alpha-C_{bridg.\ atom}$	1.324(11)	1.318(4)	1.375(7)
$C_\alpha-C_{bridg.\ atom}-C_\alpha$	121.3(8)	121.7(3)	124.9(2)
$C_\alpha-N_p-C_\alpha$	105.6(5)	106.8(2)	104.6(6)
$C_\beta-C_\alpha-N_p$	110.8(9)	110.1(3)	111.4(5)
$C_\beta-C_\beta-C_\alpha$	106.3(5)	106.5(3)	106.3(4)

[a] This work. [b] Neutron-diffraction data at 4.3 K.[18a] [c] X-ray data from ref 18b, at 295 K.

features of the in-plane parameters of Co(OESPz) are noteworthy: (i) The average $Co-N_p$ distance is much shorter than in CoOEP and, within the experimental error, slightly shorter than in CoPc. (ii) As in CoPc the $C_\alpha-N_b-C_\alpha$ bridging angle is significantly contracted relative to CoOEP. (iii) the $C_\beta-C_\beta$ bond length is shorter than in CoPc and very close to that in CoOEP.

As for the short $Co-N_p$ distance, one may wonder whether it relies on the peculiar nature of the metal−ligand interaction or is a result of the central "hole" contraction that may occur when the planar porphyrazineoctathiolato ring distorts to a ruffled conformation. Metal size and bonding seem to prevail over the ligand distortion effects in defining the structures of M^{II} (ethylsulfanyl)porphyrazines: in the case of Mn^{II} and Co^{II} (ethylsulfanyl)porhyrazines, the only complexes of transition metals with the $OESPz^{2-}$ ligand structurally characterized to date, the $M-N_p$ distances differ by 0.03 Å despite the same degree of ligand ruffling.[1h] Recent experimental and theoretical findings seem to corroborate this view. The significant differences in the $M-N_p$ bond length along the isomorphous series MOEP (M = Fe, Co, Ni, Cu) (cf. ref 18b) have also been interpreted, for instance, in terms of the prevalent effects of metal−porphyrin interaction, owing to the very similar degree of "Sad" ruffling shown by the porphyrinato core along the series. Furthermore, our previous theoretical studies on the $OESPz^{2-}$ macrocycle indicate that the "Sad" type of ruffling does not modify significantly the one-electron level pattern of the ligand relative to that observed in the planar D_{4h} symmetry and, hence, the essential features of the metal−ligand bonding interactions.[1h]

In the contraction of the $C_\alpha-N_b-C_\alpha$ bridging angle in Co(OESPz) with respect to CoOEP one may recognize a clear structural effect of the aza bridges.[3b,6] The shortening of the C_β-C_β bond lengths in Co(OESPz) and CoOEP compared to CoPc has to be ascribed, in turn, to the absence of the fused benzo rings at the β-positions.

(d) Magnetism. The temperature dependence of the magnetic susceptibility of CoOESPz measured in the range 4.2−250 K is shown in Figure 7. The value of the magnetic moment at 250 K is $\mu_{eff} = 2.08\ \mu_B$. This value is slightly higher than that expected for an $S = {}^1/_2$ spin system (consistent with a low-spin Co^{2+}) of $\mu_{eff} = 1.73\ \mu_B$.The magnetic data have been fitted using

(34) Cooper, S. R.; Rawle, S. C. *Struct. Bonding (Berlin)* **1990**, *72*, 15.
(35) Chakraborty, P.; Karmakar, S.; Kumar Chandra, S.; Chakravorty, A. *Inorg. Chem.* **1994**, *33*, 816.

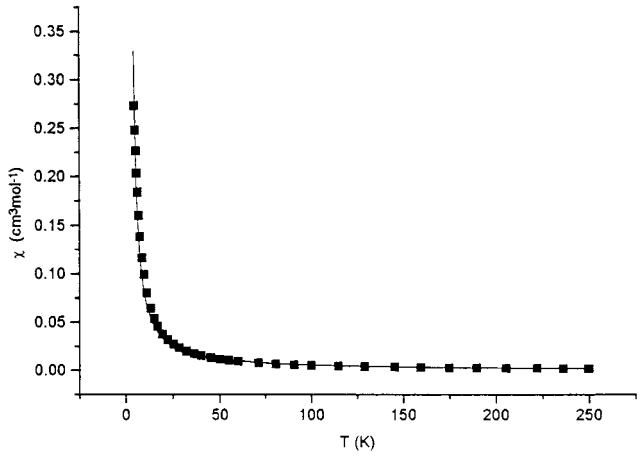

Figure 7. Temperature dependence of the magnetic susceptibility for Co(OESPz). The solid line is the best-fit curve.

a Simplex minimization routine based on the Curie−Weiss expression

$$c = \frac{C}{T - \Theta} \tag{3}$$

where

$$C = \frac{Ng^2\mu_B{}^2 S(S+1)}{3\ \mathrm{K}}$$

and Θ is the Weiss constant (in K). The expression (3) is used to describe weakly coupled magnetic systems.[36] The fitted temperature dependence of magnetic susceptibility is reported in Figure 7 as a line. The best fitted values of Θ and g are 2.6 K and 2.44, respectively.[37] The polycrystalline EPR spectra of Co(OESPz) measured in the temperature range 4.2−298 K showed a fairly isotropic signal which shifts from $g = 2.42$ at low temperature ($T = 4.2$ K) to $g = 2.28$ at room temperature ($T = 298$ K). Similar EPR spectra were obtained at low temperature ($T = 4.2$ K) in a frozen glass made from noncoordinating solvents such as CH_2Cl_2 or toluene. Both solid-state EPR and magnetic susceptibility data evidence the presence of a weak interaction between the paramagnetic Co^{2+} centers. The positive value of Θ can be ascribed to a weak ferromagnetic interaction between neighboring spin centers which accounts for the solid-state magnetic behavior of the complex. The peculiar stacking pattern shown by the Co(OESPz) molecules as well as the extraplanar Co−S interactions provide the structural basis for a possible understanding of the ferromagnetic interaction. Magnetic interaction can be ascribed to a super exchange pathway between paramagnetic metal centers mediated by the sulfanyl branches of the (ethylsulfanyl)porphyrazinato ligand with some possible participation of the π-system. Notably, Co(OESPz) is, together with Fe(OEPz), the second case of a porphyrazine-based complex showing weak intermolecular ferromagnetic coupling.[3]

Co−Macrocycle Bond in Co(OESPz) and in Related Co^{II} Tetrapyrroles, CoPc, CoPz, and CoP. (a) Electronic Structure and Bonding. The ground-state occupations corresponding to the lowest energy single determinants for CoPc, CoPz, CoP, and Co(OESPz) are shown in Figure 8. The energies have been computed using spin-unrestricted calculations, but in Figure 8 the restricted solutions are shown for sake of graphical simplicity. For CoPc, CoPz, and CoP a ground $^2A_{1g}$ state and for Co(OESPz) a ground ^2E_g state have been obtained, respectively. For Co(OESPz) the $^2A_{1g}$ state is found to lie ∼0.1 eV higher than the ^2E_g state. The calculated $S = {}^1/_2$ spin ground state is in agreement with magnetic experimental data for all systems and, in the case of CoPc and CoP, with previous calculations.[6,30a,38]

The energy of the one-electron levels changes significantly with the macrocycle framework. In the series CoP, CoPz, CoPc, and Co(OMSPz) one can easily recognize the effect of introducing in the porphyrin ring aza bridges (CoP → CoPz) and peripheral substituents, i.e., benzo rings (CoPz→CoPc) and a $(MeS)_8$ cage (CoPz → Co(OMSPz)). Introducing the aza bridges, in CoPz, stabilizes all the one-electron levels due to the higher nuclear charge of N but preferentially the $2a_{2u}$ which ends up considerably below the $1a_{1u}$. This fits in with the $2a_{2u}$ having high amplitude on aza bridges (it is actually mainly composed of N_p and N_b $2p_z$). The major effect of the introduction of benzo rings, in CoPc, is to destabilize the $1a_{1u}$, a pure π ligand orbital mainly located on the pyrrolic rings, notably the C_α atoms, which in CoPc ends up above the $2a_{2u}$ and all metal orbitals. The pushing-up effect of benzo rings is due to the antibonding between the pyrrolic part of the ring system and the benzo part. The large stabilization of the $2a_{2u}$ on going from CoPz to CoPc (in CoPc it is even the lower lying $1a_{2u}$ rather than the $2a_{2u}$ which correlates with the $2a_{2u}$ of CoPz) can simply be ascribed to the enlargement of the porphyrazinic core which causes a decrease of the N_p-N_b antibonding.

The effect of adding sulfur atoms at the β-positions of Pz, shown by Co(OESPz), is to destabilize all the levels but preferentially the $1e_g$ and $2e_g$, the latter becoming the HOMO of the molecule. These two orbitals are, in all complexes of the series, the bonding and antibonding combinations of Co-d_π and the highest ligand-$\pi(e_g)$ orbital, in accordance with the antibonding, visible in the plots of the Co(OMSPz) $1e_g$ and $2e_g$. As shown in Figure 9, these orbitals are antibonding with respect to the porphyrinic part and the S-$3p_z$ which contribute to these orbitals not less than 30%. The antibonding interaction with the S-$3p_z$ atomic orbital destabilizes also the eg* which ends up at the same energy as in CoP, although the pushing up effect of the sulfur atoms is less pronounced than in the lower lying $2e_g$ and $1e_g$, due to the smaller contribution (11%) of the S-$3p_z$.

The computed dependence of the Co^{II} tetrapyrrole one-electron energy levels on changes in the macrocycle framework raises the question about possible differences in the metal−ligand interactions along the series, a point that we will discuss in some detail.

Among the orbitals shown in Figure 8 and labeled according to D_{4h} notation, the b_{1g}* ($d_{x^2-y^2}$), the doubly degenerate $1e_g$ (d_π) and $2e_g$ (d_π), the $1a_{1g}$ (d_{z^2}), and the $1b_{2g}$ (d_{xy}) and $2b_{2g}$ (d_{xy}) involve the metal to a significant extent.

The b_{1g}* orbital is essentially a $Co-N_p$ antibonding state composed by Co-$d_{x^2-y^2}$ and pyrrolic nitrogen lone pairs in almost equal amount. Its bonding counterpart, not shown in the figure, is much lower in energy because of the strong σ interaction. The energy gap between the bonding/antibonding pair is 6.06, 6.78, 7.70, and 7.74 eV for CoP, CoPc, Co(OMSPz) and CoPz, respectively, indicating a stronger $Co-N_p$ interaction in the *meso*-tetraaza-substituted metallomacrocycles. This is reasonable in view of the larger Co/N_p overlap due to the shortening of the $Co-N_p$ distance (see Table 3). The data of Table 4, where

(36) Chakravarty, A. S. *Introduction to the Magnetic Properties of Solids*; Wiley: New York, 1980.
(37) Press, W. H.; Flannery, B. P.; Teukolsky, S. A.; Vetterling, W. T. *Numerical Recipies, Fortran Version*; Cambridge University Press: New York, 1989.
(38) Reynolds, P. A.; Figgis, B. N. *Inorg. Chem.* **1991**, *30*, 2294.

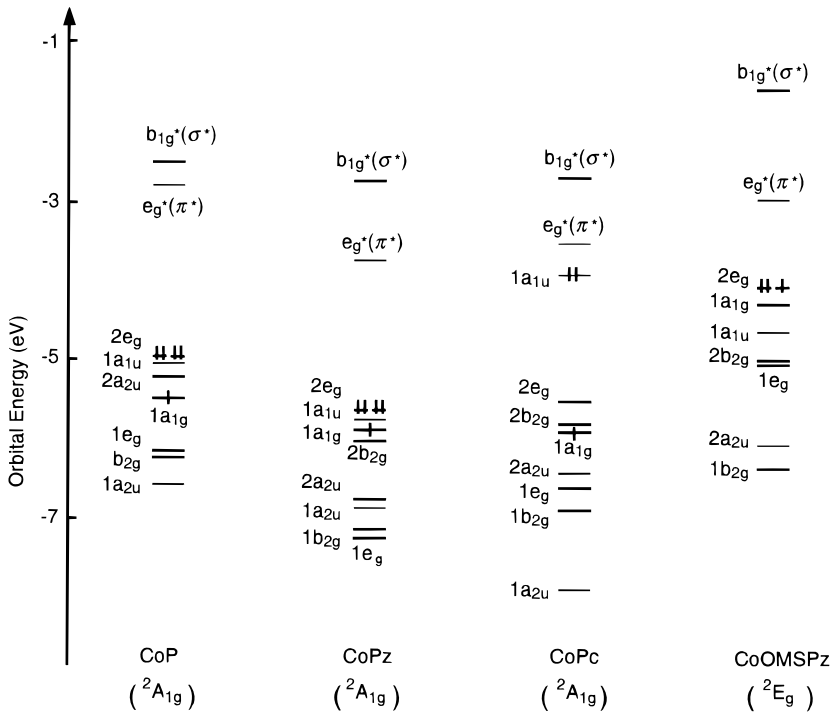

Figure 8. Energy levels for the CoP, CoPz, CoPc, and Co(OMSPz) series obtained from spin-restricted calculations. Only the orbitals near the Fermi level are shown. All the orbitals below the HOMO ($2e_g$ for CoP, CoPz, and Co(OMSPz) and $1a_{1u}$ for CoPc, respectively) are fully occupied, if not shown, and those above the HOMO are empty. The heavy lines indicate the orbitals which are predominantly of metal character.

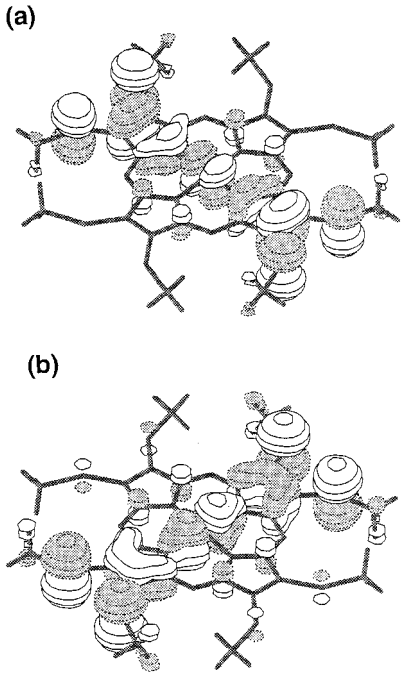

Figure 9. Isosurface plot of Co(OESPz) (a) $2e_g$ and (b) $1e_g$ orbitals (orientation of the molecule as in Figure 1). The value of th surface corresponds to 0.05 $(e/bohr^3)^{1/2}$.

the Mulliken gross population of SCF orbitals of Co and tetrapyrrole fragments in the Co(II) tetrapyrrole series are given, confirm the strong interaction in B_{1g} symmetry. They show indeed that the largest charge transfers occur in this symmetry: 0.81, 0.82, 0.85, and 0.86 electrons are donated to cobalt from the b_{1g} N_p lone pair of P, OMSPz, Pc, and Pz, respectively. The situation in this symmetry is actually close to a homopolar electron pair bond between metal and ring.

The $1a_{1g}$ is mainly a pure metal orbital, largely (∼85%) d_{z^2} with some (∼9%) 4s character and a small admixture of ligand

Table 4. Mulliken Gross Population of SCF Orbitals of L (L = P, Pz, Pc, OMSPz) and Co Fragments in CoP, CoPz, CoPc, and Co(OMSPz), Where All Virtual Orbitals of a Given Symmetry Are Collectively Denoted by a Prefix "*n*"

Γ			CoP ($^2A_{1g}$)	CoPz ($^2A_{1g}$)	CoPc ($^2A_{1g}$)	Co(OMSPz) (^2E_g)
A_{1g}	Co	4s	0.32	0.30	0.30	0.41
		$3d_{z^2}$	1.01	1.02	1.02	1.86
		nd_{z^2}	0.01	0.01	0.00	0.01
	L	a_{1g}	1.68	1.70	1.70	1.72
		na_{1g}	0.00	0.00	0.00	0.00
B_{1g}	Co	$3d_{x^2-y^2}$	0.74	0.79	0.79	0.75
		$nd_{x^2-y^2}$	0.07	0.07	0.07	0.07
	L	b_{1g}	1.18	1.17	1.15	1.17
		nb_{1g}	0.00	0.00	0.00	0.02
B_{2g}	Co	$3d_{xy}$	1.95	1.94	1.94	1.93
		nd_{xy}	0.02	0.02	0.02	0.02
	L	b_{2g}	2.00	2.00	1.99	2.00
		nb_{2g}	0.03	0.00	0.05	0.05
E_g	Co	$3d_{\pi}$	3.80	3.72	3.74	3.04
		nd_{π}	0.04	0.04	0.04	0.04
	L	e_g	3.94	3.98	3.90	3.40
		ne_g	0.24	0.26	0.32	0.52
A_{2u}	Co	$3p_z$	2.00	2.00	2.00	2.00
		$4p_z$	0.08	0.09	0.08	0.07
	L	a_{2u}	1.92	1.93	1.89	1.91
		na_{2u}	0.03	0.00	0.04	0.02
E_u	Co	$3p_{\sigma}$	3.98	3.98	3.98	3.98
		$4p_{\sigma}$	0.38	0.32	0.34	0.26
	L	e_u	3.66	3.76	3.76	3.76
		ne_u	0.00	0.00	0.00	0.00

a_{1g} type orbitals. According to the fragment populations in A_{1g} a ligand to metal σ donation occurs in this symmetry. In all complexes of the series ∼0.3 electrons are transferred from the ligand-a_{1g} to the 4s atomic orbital of the metal. In Co(OMSPz) the 4s also picks up some charge from the fully occupied $3d_{z^2}$. The $1b_{2g}$ and $2b_{2g}$ MOs account, in CoPz, CoPc, and Co(OMSPz), for the bonding and antibonding π in-plane interaction between the cobalt d_{xy} and the highest occupied b_{2g} orbital of the *meso*-azamacrocycles, which is mostly a N_b lone pair orbital

but also contains some N_p in-plane p_π. According to the populations in Table 4, the occupied Co-d_{xy} mixes very little with virtual orbitals of the tetrapyrrole ligand of this symmetry which lie at too high energy. The π in-plane interaction is therefore primarily a two-orbital four-electron repulsive interaction. In CoP the d_{xy} is found almost purely in the $1b_{2g}$ MO (see Figure 8). The reason is that, due to the replacement of the aza bridges by methinic bridges, the highest occupied P-b_{2g} orbital is downward shifted and is no longer suitable for π in-plane interaction with the Co-d_{xy}.

The $2e_g$ molecular orbital is heavily mixed with the highest occupied ligand-$\pi(e_g)$ orbital which, owing to a sizable N_p p_z character, is suitable for out-of-plane interaction with the Co-d_π orbitals. Its bonding counterpart is the $1e_g$. In the $1e_g/2e_g$ pair the metal contribution in the $2e_g$ decreases along the series (70% in CoP, 56% in CoPc, 54% in CoPz, and 41% in Co(OMSPz)) and increases in the $1e_g$ (23% in CoP, 29% in CoPc, 34% in CoPz, and 35% in Co(OMSPz)) due to the changes in the relative Co-d_π and ligand-$\pi(e_g)$ energies.

Not only the composition but also the spacing of the π bonding/antibonding pair $1e_g/2e_g$ changes along the series, though not monotonically with the decrease of the Co−N_p distance. The energy gap amounts indeed to 1.69, 1.40, 1.74, and 0.94 eV in CoP, CoPc, CoPz, and Co(OMSPz), respectively, indicating that, despite the same Co−Np distance, the $1e_g/2e_g$ splitting is in Co(OMSPz) about half of that in CoPz. The observed trend is determined by the amount of N_p p_z character of the ligand-$\pi(e_g)$ orbital interacting with the Co-$3d_\pi$ rather than by the Co−N_p distance. We find for instance that the OMSPz-$\pi(e_g)$ contains only a 18% of N_p p_z to be compared with a 38% of the Pz-$\pi(e_g)$.

It is noteworthy that the mixings that occur in e_g type orbitals mainly involve occupied ligand-$\pi(e_g)$ orbitals, almost exclusively the highest occupied one, leading to a two-orbital four-electron destabilizing interaction. In Co(OMSPz) where the antibonding $2e_g$ orbital is partially occupied this interaction can be considered as a two-orbital three-electron interaction. In such cases the antibonding contribution most of the time largely cancels or even outweighs the bonding contribution. The participation of the lowest lying $\pi(e_g)$ virtual into the $2e_g$ is small but not negligible, especially in Co(OMSPz), where it is 12%. The π back-donation of the filled d_π into the virtual ligand-e_g* amounts to 0.16, 0.24, and 0.22 electrons in CoP, CoPz, and CoPc, respectively. In Co(OMSPz) no metal to ligand π back-donation occurs; some charge (0.08 electrons) flows instead from the occupied ligand-$\pi(e_g)$ orbitals into the Co-d_π.

The populations in Table 4 indicate that a sizable polarization of the ligand occurs in E_g symmetry. In CoP, CoPz, CoPc, and Co(OMSPz) 0.08, 0.02, 0.10, and 0.52 electrons, respectively are transferred from the highest occupied ligand-$\pi(e_g)$ orbital into the empty ligand-$\pi(e_g)$ orbitals. In Co(OMSPz) this is actually the only relevant charge rearrangement.

A charge rearrangement also occurs in A_{2u} and E_u symmetries. In A_{2u}, the Co-$4p_z$ slightly mixes with the highest occupied ligand-$\pi(a_{2u})$ orbital in the $1a_{2u}$ and/or $2a_{2u}$ MOs of the Co^{II} tetrapyrroles. The resulting $4p_z$ population is accordingly quite small (less than 0.1 electrons). A significant σ ligand to metal charge transfer (0.24 and 0.34 electrons are acquired by the Co-$4p_\sigma$ in the *meso*-tetraazamacrocycles and in CoP, respectively) occurs on the contrary in E_u symmetry although the mixing of the Co-$4p_\sigma$ with the low-lying N_p σ-lone pair combinations of E_u symmetry is quite small (∼5%).

(b) Metal−Macrocycle Bonding Energies. We have performed a quantitative energy analysis of the metal−ligand interactions in the Co^{II} tetrapyrrole series using the decomposition scheme discussed in the Computational Details section. The results are reported in Table 5.

Table 5. Decomposition of the Bonding Energy for Co^{II} Tetrapyrrole Complexes (Tetrapyrrole = P, Pz, Pc, OMSPz) in Terms of Co^{2+} and Tetrapyrrole(2−) Ionic Fragments with All Data from Spin-Unrestricted Calculations

	CoP[a] ($^2A_{1g}$)	CoPz ($^2A_{1g}$)	CoPc ($^2A_{1g}$)	Co(OMSPz) (^2E_g)
ΔE_{Pauli}	+7.77	+10.28	+9.53	+10.55
ΔE_{elstat}	−27.30	−27.84	−26.02	−26.05
ΔE^0	−19.53	−17.56	−16.49	−15.50
$\Delta E^{A_{1g}}$	−3.18	−3.28	−3.14	−2.25
$\Delta E^{B_{1g}}$	−6.73	−7.48	−7.03	−7.61
$\Delta E^{B_{2g}}$	−0.65	−0.78	−0.69	−0.81
ΔE^{E_g}	−1.80	−1.90	−2.51	−4.07
$\Delta E^{A_{2u}}$	−1.02	−1.00	−1.22	−0.94
ΔE^{E_u}	−3.04	−3.22	−2.87	−3.40
ΔE^{nb}	−1.33	−1.47	−1.89	−1.54
ΔE_{oi}	−17.75	−19.13	−19.35	−20.62
$\Delta E_{\text{oi}} + \Delta E^0$	−37.28	−36.69	−35.84	−36.12

[a] Data from spin-unrestricted calculations. The open-shell fragment method has been used.[27]

To have a clear and meaningful energy contributions in the individual irreducible representations, we promote the fragments to the ionic configurations tetrapyrrole(2−) and Co^{2+} [Co, $d_{x^2-y^2}{}^0 d_\pi{}^3 d_{z^2}{}^2 d_{xy}{}^2 4s^0$ in the case of Co(OMSPz); Co, $d_{x^2-y^2}{}^0 d_\pi{}^4 d_{z^2}{}^1 d_{xy}{}^2 4s^0$ in the case of CoP, CoPz, and CoPc].

It should be noted that our analysis refers to the final situation, with the bonds formed. This change of configuration has the advantage that the Pauli repulsion due to 4s disappears. The $d_{x^2-y^2}$ is emptied and acts as acceptor orbital for electrons from the occupied ligand(2−)-b_{1g} orbital.

Looking first at the steric term, ΔE^0, which can be considered as a measure of the "ionic" contribution to the bonding, we note that it is strongly attractive in all complexes of the series, due to the fact that the stabilizing contribution arising from the large attractive interaction between charged fragments, ΔE_{elstat}, overcomes the positive (destabilizing) Pauli repulsion term, ΔE_{Pauli}. As shown in Table 5, the steric interaction energy is very sensitive to the nature of the macrocycle, being in CoPz and specially CoP (*small ring* macrocycles) considerably more negative than in CoPc (*large ring* macrocycle) and Co(OMSPz) (*peripherally substituted small ring* macrocycle). The contributions to the steric term reveal that the electrostatic component becomes more attractive in the order CoPz > CoP > CoPc ∼ Co(OMSPz). This is still an effect of the macrocycle framework, in the sense that is due to the fact that the charge density on P^{2-} and especially on Pz^{2-} is higher than on Pc^{2-} and $OMSPz^{2-}$ where the charge delocalization is more effective.

The repulsive ΔE_{Pauli} term increases in the order CoP ≪ CoPc < CoPz ∼ CoOMSPz, reflecting the decrease of the hole size in the macrocycles and hence the increase of the Pauli repulsion between the closed-shell electrons on the interacting fragments.

Considering the individual contributions to the orbital interaction term, ΔE_{oi}, it is apparent from the data of Table 5 that the $\Delta E^{B_{1g}}$ term which accounts for σ-donation into the Co-$d_{x^2-y^2}$ orbital is by far the largest one, in line with the large charge transfer observed in B_{1g} symmetry (cf. Table 4). The $\Delta E^{B_{1g}}$ values along the series clearly show that the stronger the σ-donation, the shorter the Co−N_p distance. This fully corroborates previous suggestions that tetraazaporphyrins are stronger Lewis bases than porphyrins and phthalocyanines.

A relevant contribution to the σ bond also comes from the $\Delta E^{A_{1g}}$ and ΔE^{E_u} terms, reflecting the sizable charge transfer into

4s and 4p_σ, respectively, by ring orbitals, whereas, as expected, the $\Delta E^{B_{2g}}$ term is very small.

As for the energy terms which account for the π-bond, the $\Delta E^{A_{2u}}$ is small, in accordance with the little charge transfer observed into the Co-4p_z.

The most relevant contribution to the π interaction comes from the ΔE^{E_g} term. In the investigated series where a genuine electron pair bond is not being formed since the interactions in this symmetry give rise to four-electron two-orbital or three-electron two-orbital repulsive interactions, the ΔE^{E_g} term only accounts for the π-back-donation from the d_π into the empty ligand-π^* orbitals and for polarization effects.

From the data reported in Table 5, we note that the ΔE^{E_g} term is in Co(OMSPz) where π-back-donation is not present, very large, more than two times larger than in CoP and CoPz. This result suggests that polarization of the macrocycle (in Co(OMSPz) it amounts to 0.52 electrons) is energetically not less important than π-back-donation. Previous calculations on MPcs (M = Mg, Co, Ni, Cu)[6] have shown that polarization of the macrocycle can be energetically even more important than π-back-donation.

We have collected in the term ΔE^{nb} the energetic contributions arising from the A_{2g}, A_{1u}, B_{1u}, and B_{2u} symmetries. Since there are no metal orbitals which transform according to these irreducible representation, the interaction energies in these "nonbonding" symmetries represent pure polarization, arising from empty/occupied orbital mixing on the ligand. The energetic effect of the polarization is relatively small (between 1.2 and 1.9 eV in these symmetries) but not negligible.

The total orbital contribution (covalent component) is stabilizing in all investigated complexes, being the largest in Co(OMSPz) and, except in CoP, prevails over the ionic component.

The total bonding energy (ΔE^0 and ΔE_{oi}) values indicate that Co^{2+} is strongly bound to the ligand(2−). Bonding in CoP is slightly stronger than in the *meso*-tetraaza-substituted porphyrins, despite weaker orbital interactions, due to a more negative steric term caused by both a smaller Pauli repulsion and a stronger electrostatic attraction.

Concluding Remarks

The newly synthesized complex Co(OESPz) forms, similarly to the isomorphous Mn(OESPz), solid-state extended one-dimensional aggregates where "ruffled" molecular units are held together by extra planar Co···S interactions, which open, probably with the contribution of the π system, a superexchange path for intermolecular ferromagnetic interactions between the low-spin Co^{2+} ($S = {}^1/_2$) centers.

The molecular structural features of the porphyrazinato core as well as the electrochemical properties of the complex are typical of metallotetraazaporphyrins. Co(OESPz) shows indeed a Co−N_p bond length shorter than CoOEP and even than CoPc and a sensible electrochemical stabilization of the Co(III) over the Co(III) state.

Electronic structure calculations of the title complex and of related Co^{II} tetrapyrroles show that the ligand framework strongly influences the energy of the one-electron levels. It is found, in particular, that the aza bridges stabilize all levels.

Similarities and differences between CoPc and Co(OMSPz) have been highlighted by discriminating the effects of benzo rings and the $(MeS)_8$ cage on the porphyrazine ring. Introducing benzo rings at the periphery of the porphyrazinato ring has the only effect of destabilizing the a_{1u} ligand obital which becomes the HOMO of CoPc, whereas addition of a $(MeS)_8$ cage shifts up all levels, especially the e_g type orbitals, counteracting the stabilizing effect of the aza bridges.

The detailed energy analysis of the metal−macrocycle interactions in the Co^{II} tetrapyrrole series points out that in the aza-bridged complexes, particularly in CoPz and Co(OMSPz), the reduced hole size increases the σ interactions which are by far dominant in all members of the series, mostly due to strong charge donation from the pyrrolic nitrogen lone pairs to the empty Co-$d_{x^2-y^2}$ with additional effects from donation into the 4$p_{x,y}$ and 4s.

The π interactions, consisting of π-back-donation from 3d_π into empty ring π orbitals and donation from the occupied ring π orbitals into the Co-4p_z and polarization of the macrocyclic ligand, are much weaker than σ interactions in all complexes.

At variance with the accepted view, the aza bridges have little effect on the metal to ligand π-back-donation, which is in the series rather weak or, as in the case of Co(OMSPz), completely absent.

The role played by the peripheral substituents in the metal-macrocycle π interactions is much more relevant so. The benzo rings and thioether groups are responsible indeed for the large polarization effects observed in CoPc and especially in Co(OMSPz) where the ΔE^{E_g} term, which in this case only accounts for polarization effects, is the largest in the series.

The total orbital interaction contribution (covalent component) prevails over the ionic component of the bond in all porphyrazines (which is very large indeed in CoPz) but especially in Co(OESPz), due to the strong polarization effects induced by the peripheral substituents which make the ΔE_{oi} term the largest in the series.

Acknowledgment. Thanks are expressed to Dr. A. Caneschi, University of Firenze, for performing magnetic measurements and to Dr. E. Giannasi for the help in the structural investigation. Thanks are due to the Servizio di Spettrometria di Massa, University of Napoli, for performing FAB mass spectra and to Prof. P. Pucci for helping in their interpretation, to Mr. S. Laurita for collecting X-ray data, and to Mr. C. Barlabà for technical support. The financial support from Ministero della Università e della Ricerca Scientifica e Tecnologica (MURST) and from Consiglio Nazionale delle Ricerche (CNR) is also gratefully acknowledged.

Supporting Information Available: Tables S1−S6, listing complete data collection information, hydrogen positional and thermal parameters, interatomic distances and angles, anisotropic thermal parameters, least-squares plane, and intermolecular contacts within 4 Å. This material is available free of charge via the Internet at http://pubs.acs.org.

IC9811547